

## Variation of flow separation over large bedforms during a tidal cycle

A. Lefebvre<sup>(1)</sup>, Y. Ferret<sup>(1)</sup>, A.J. Paarlberg<sup>(2)</sup>, V.B. Ernstsen<sup>(3)</sup> and C. Winter<sup>(1)</sup>

1. MARUM – Center for Marine Environmental Sciences, Bremen, Germany -  
alefebvre@marum.de

2. HKV Consultants, Lelystad, The Netherlands.

3. Department of Geosciences and Natural Resource Management, University of Copenhagen, Denmark

### Abstract

This study characterizes the shape of the flow separation zone over natural compound bedforms during a tidal cycle and investigates how the flow separation zone depends on changing flow conditions, water levels and bathymetry. Field data collected during a full tidal cycle over large ebb-oriented bedforms provides high-resolution bathymetry and velocity measurements that are used to simulate the hydrodynamics structure during a tidal cycle using the Delft3D numerical model.

During the ebb, a large flow separation zone occurs on the steep lee side (14 to 23°) of each bedform. During the flood, no flow separation developed over the gentle slope of the flood lee side (3 to 5° on average). However, a small flow separation zone is often recognized near the crest, where the slope is locally up to 15°. The shape of the FSZ is not influenced by changes in current velocities or water levels. On the contrary, it is largely influenced by changes in the bed morphology. In particular, variations in the shape of the crest during the tidal cycle results in variations of the length of the FSZ.

### 1. INTRODUCTION

In tidal inlets and rivers, strong currents and high availability of sandy sediment result in large asymmetric bedforms (having a gentle and a steep side, Figure 1). If the bedform lee slope is steep enough, the pressure gradient at the edge of the bedform crest creates flow separation and the formation of a recirculating eddy is induced within the Flow Separation Zone (FSZ, Figure 1). This FSZ has a strong influence on the resistance that bedforms exerts on the flow due to energy loss through turbulence (Vanoni and Hwang, 1967). Furthermore, it complicates sediment transport above bedforms due to the presence of reverse flow within the FSZ. It is therefore highly relevant for the understanding and modeling of coastal hydro- and sediment dynamics to determine the length and shape of the FSZ for different flow conditions.

The FSZ has been widely studied over bedforms with a lee side close or equal to the angle-of-repose (~30°) which commonly occurs in rivers (see review by Best, 2005). Over such bedforms, a

permanent FSZ develops. However, bedforms with a lee side smaller than the angle-of-repose have also been observed to commonly occur in rivers (e.g. Best and Kostaschuk, 2002) and in tidal environments (e.g. Lefebvre et al., accepted). The FSZ over lee sides that are less steep than the angle-of-repose is thought to be non-existent or intermittent. However, the exact slope at which the FSZ becomes permanent has not yet been determined. Paarlberg et al. (2009) considered that flow separation is permanent in time for a slope of 10° or more. Kostaschuk and Villard, (1996) suggested that flow separation may occur intermittently only for lee side slopes up to 19° and Best and Kostaschuk (2002) found that flow separation over bedforms with maximum lower lee side slope of 14° was present for about 4% of the time.

In tidal environments, flow reverses depending on the tidal phase and large bedforms usually keep their asymmetry, typically being oriented with the residual flow direction (e.g. Ernstsen et al., 2006). Therefore, their lee side may be steep or gentle depending on the tidal phase (Figure 1) which

implies that the FSZ varies depending on flow direction. Furthermore, the angle of the steep side of tidal bedforms is often smaller than the angle of repose (typically between 10 and 20°) i.e. in the range of angles over which the presence of a permanent FSZ is still under debate. In addition, the influence on the FSZ of tidally-induced variations of flow velocity, water level and bathymetry is still to be determined; in other words, the effect on the FSZ of tidal flow acceleration and deceleration, tidal range and variations of bathymetry due to sediment movement during a tidal cycle is unknown. This is largely due to the difficulty, if not impossibility, to measure the near-bed flow over bedforms in a natural environment.

This study aims, through numerical modeling, at characterizing the shape of the FSZ over natural asymmetric bedforms during a tidal cycle and investigating how the FSZ varies with changing flow velocities, water levels and bathymetry.

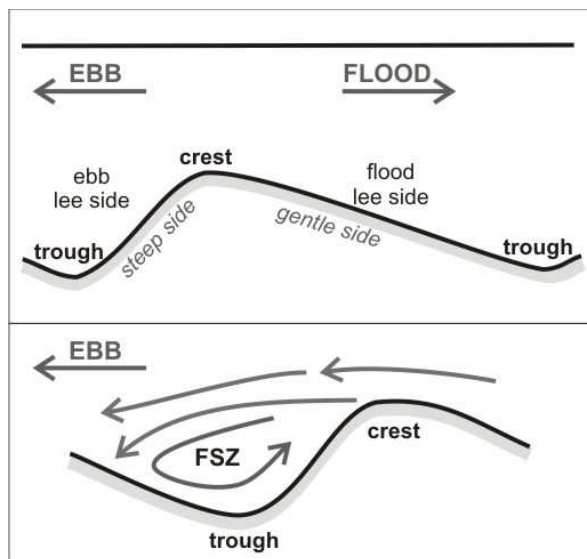


Figure 1. Top: sketch of an asymmetric bedform in a tidal environment; bottom: detail of the Flow Separation Zone (FSZ).

## 2. METHODS

### 2.1. Study area

The Knudedyb tidal inlet connects a tidal basin of the Danish Wadden Sea to the adjacent North Sea. The Knudedyb channel is around 8.5 km-long and

1 km-wide with an average water depth of about 15 m (Figure 2). The tides in the area are semi diurnal with a tidal range of 1.6 m on average. The tidal inlet bed is sandy and covered with compound bedforms (Lefebvre et al., 2011): large ebb-oriented bedforms (wavelengths of several hundred meters and heights of several meters) on which smaller bedforms (wavelengths of 3 to 5 m and heights of 0.15 to 0.3 m) are superimposed. These secondary bedforms reverse directions and migrate in the direction of the tidal currents while the primary bedforms stay ebb-oriented throughout the tidal cycle.

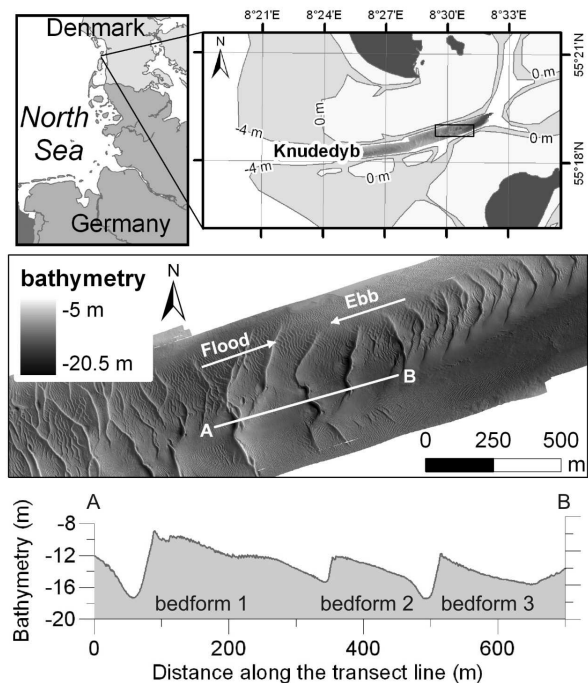


Figure 2. Top: location of the Knudedyb tidal channel and configuration of the inlet. Middle: bathymetry (m under mean sea level) around the measurement site and location of the transect line. Bottom: bed elevation profile along the transect line.

### 2.2. Field data

Repetitive surveys were conducted over a 700 m-long transect line crossing 3 primary bedforms (Figure 2) with the RV Senckenberg on 17 October 2009 during a full tidal cycle (Lefebvre et al. accepted). Flow velocity magnitudes and directions were measured using an acoustic Doppler current profiler (ADCP) operating at 1200

kHz and the seabed bathymetry was recorded using a high-resolution multibeam echosounder (MBES) operating at 455 kHz. The measurements of seabed bathymetry and flow velocity were performed simultaneously while the vessel was moving against the main tidal current in order to maintain a straight course at a constant and relatively low vessel speed. A total of 16 repetitive runs were carried out.

The ADCP data were used to calculate transect-averaged water levels and depth-averaged velocity magnitude and direction (Figure 3). The tidal range during the survey was 1.8 m. During the flood, the flow direction was  $66^\circ$  N on average (ESE to WNW) and (transect and depth-averaged) maximum velocity was 0.9 m/s. During the ebb, the flow direction was  $242^\circ$  (WNW to ESE) and (transect and depth-averaged) maximum velocity was 1.1 m/s (Lefebvre et al. accepted).

The bathymetric data were gridded with a cell size of  $0.5 \times 0.5$  m and bed elevation profiles (BEPs) were extracted from the gridded bathymetry along the transect line. The troughs and crests of the large bedforms were determined following Ernstsens et al. (2010) as the lowest and highest elevation along each bedform and used to calculate bedform dimensions.

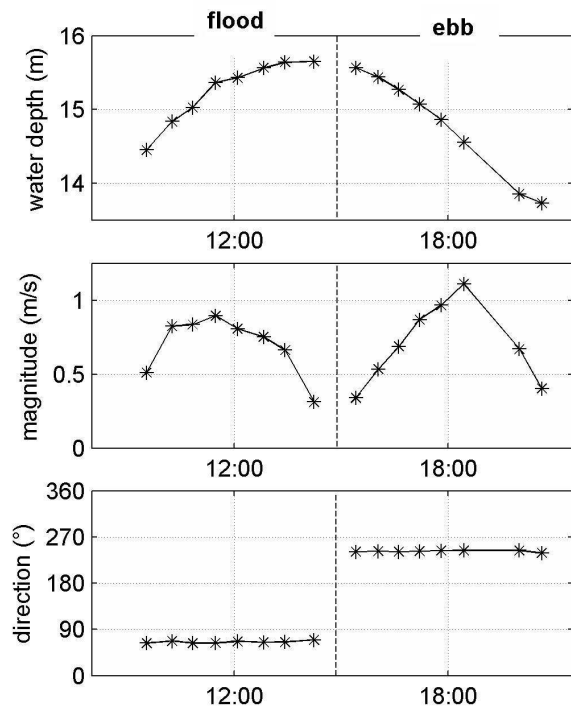


Figure 3. Variations of water depth and transect- and depth-averaged velocity magnitude and direction recorded by the ship mounted ADCP.

### 2.3. Numerical model

Delft3D (Deltares, 2011) is a process-based open-source integrated flow and transport modeling system. In Delft3D-FLOW the 3D non-linear shallow water equations, derived from the three dimensional Navier-Stokes equations for incompressible free surface flow, are solved. In order to capture the flow circulation above bedforms, the non-hydrostatic version and the k-epsilon turbulence closure are used.

The numerical model has been calibrated and validated against velocity and water level data from the laboratory flume experiments of McLean (1999). It proved to be able to correctly reproduce flow separation over bedforms, in particular the shape and length of the FSZ (Lefebvre et al., 2012).

### 2.4. Model Experiments

Five experiments were carried out using the numerical model. All simulations were done with the hydrodynamic module (without sediment transport) using velocity as entrance boundary condition and water level as exit boundary conditions. The horizontal grid cell was set to 0.5 m and the vertical grid was composed of 59 non-equidistant layers having a size of 0.2 m between the lowest and highest point of the bed profile (i.e. lowest trough and highest crest), before gradually increasing to a size of 1 m in the water column. The time step was 0.01 second.

The five experiments (Table 1) were designed to investigate the effects of changes in flow velocity, water levels and morphology on the FSZ.

The velocity setting was defined as (a) steady: 16 steady flow simulations were carried out, each simulation using one of the 16 velocity magnitudes calculated from the field data (Figure 3) or (b) tidal: one simulation was carried out with tidally-varying velocity magnitude.

The water level setting was defined as (a) mean: the water level was constant and equal to the mean water level recorded during the field survey, (b) varying: the water level was constant and varied to match the field data or (c) tidal: the water level was tidally-varying.

The morphology setting was defined as (a) mean: the bathymetry used was the mean bathymetry of

the field bathymetry data or (b) varying: each simulation was carried out using one of the 16 field bathymetries.

Table 1. Summary of the simulations carried out with details of the experiment number (exp. number) and the number of simulations for each of these experiments (number of sim.).

| Exp. number | Number of sim. | Velocity | Water level | Morphology |
|-------------|----------------|----------|-------------|------------|
| 1           | 16             | steady   | mean        | mean       |
| 2           | 1              | tidal    | mean        | mean       |
| 3           | 16             | steady   | varying     | mean       |
| 4           | 1              | tidal    | tidal       | mean       |
| 5           | 16             | steady   | varying     | varying    |

## 2.5. Flow separation zone

The precision of the field data being insufficient to accurately determine the position of the FSZ (Lefebvre et al, accepted) the present study concentrates on characterizing the FSZ from the numerical simulation experiments. The method used to determine the presence and shape of the FSZ was adapted from Paarlberg et al. (2007) and Lefebvre et al (2012). The FSZ was sought on the lee of each bedform for each simulation as follow (Figure 4):

- the profiles with negative velocity were found
- the height of zero velocity point was calculated along each velocity profile
- the zero velocity line was determined and parameterized. It was observed to be composed of two segments: (1) upper zero velocity line: over the slip face, i.e. from the first profile with a negative velocity until the profile where the angle of the bed became higher than  $-12^\circ$  (MID), the zero velocity line was a straight line and was fitted with a 1<sup>st</sup> order polynomial and (2) lower zero velocity line: over the trough and stoss side (angle of the bed profile  $> -12^\circ$  until last profile with negative velocity) the lower zero velocity line was fitted with a 3<sup>rd</sup> order polynomial
- the intersection between the upper segment of the zero velocity line and the bed defined the separation point (SEP, beginning of the FSZ)
- the separation points were calculated along each profile by calculating the height at which the integral of the velocity between the bed and that point is zero (see Paarlberg et al. 2007)
- the flow separation line was calculated by fitting a 3<sup>rd</sup> order polynomial through the flow

separation points, assuming that this polynomial went through the separation points

- the reattachment point (RET) was defined as the point where the flow separation line crossed the bed
- the height of the FSZ ( $H_{FSZ}$ ) was calculated as the height between the separation point and the trough
- the extent of the FSZ ( $L_{FSZ}$ ) was the horizontal distance between the separation point and the reattachment point
- the normalized extent of the FSZ was calculated,  $L'_{FSZ} = L_{FSZ} / H_{FSZ}$

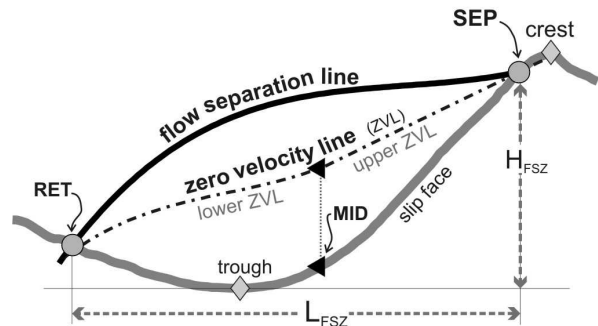


Figure 4. Schematic of the FSZ; SEP = separation point; MID = “middle” of the zero velocity line, i.e. profile where the angle of the bed is higher than  $-12^\circ$ ; RET = reattachment point;  $H_{FSZ}$  = height of the flow separation zone;  $L_{FSZ}$  = length of the FSZ.

## 3. RESULTS

### 3.1. Overall difference between ebb and flood

Based on the results of all experiments, it is observed that during the ebb a FSZ is present on the steep lee side of all three bedforms (Figure 5). The normalized length of the FSZ was on average 5.7 over bedform 2, and 6.2 over bedforms 1 and 3. Bedform 2 has a complicated morphology near the crest making the flow separates at the edge of the slip face and not close to the crest (highest point along the bedform). Therefore, in this case, the crest is defined as the last point before the trough which has positive bed slope (Figure 5).

In most cases during the flood, no FSZ develops over the gentle lee side, due to the flat bed at the crest (Figure 6). However, a small FSZ is sometimes recognized over the steepest part of the bedform, in general over bedform 1 (Figure 6). This FSZ has a normalized length of 1.3. This

small value shows that this FSZ is not related to the whole bedform but only to the steepest part of the bed near the crest.

### 3.2. Influence of velocity

Experiments 1 and 2 were designed to test the effect of velocity on the FSZ, specifically whether changes in steady velocity (Exp. 1) or tidally-varying (unsteady) velocity (Exp. 2) influence the length of the FSZ. The results of Experiments 1 and 2 reveals no effects of velocity on the FSZ. The variations in the FSZ during the tidal cycle are due to flow reversal with a small or non existent FSZ during the flood and a permanent well developed FSZ during the ebb (as outlined in Section 3.1.). During the ebb, the FSZs are clearly developed when flow velocity magnitudes becomes larger than  $0.2 \text{ m s}^{-1}$  (around 20 min after slack water) and stable until flow reversal impacts the velocity directions and hence a clear FSZ can not be distinguished (around 20 min before slack water).

### 3.3. Influence of water level

Experiments 3 and 4 were performed to test the influence of changing water levels on the FSZ. During the tidal cycle simulated here, the tidal range is 1.8 m (Figure 3) and the relative bedform height (bedform height / mean water depth) varies from 0.52 to 0.59 (bedform 1), 0.22 to 0.25 (bedform 2) and 0.34 to 0.39 (bedform 3). The results show that varying water levels has no influence on the FSZ. Furthermore, bedforms 1 and 3 have a similar normalized length of FSZ despite having different relative height implying that relative height is not a determining factor of the normalized length of the FSZ.

### 3.4. Influence of morphology

Experiment 5 was designed to test the effect of the changes in morphology on the FSZ. The high-resolution MBES data collected during the field campaign provided bathymetric data that realistically depicted the changes in bathymetry due to sediment transport during a tidal cycle. The troughs of the bedforms did not change significantly during the tidal cycle, whereas the crests were clearly altered by sediment movement. In particular, the crest of bedform 1 developed a flood cap during the flood, i.e. a high and steep

crest, which then disappeared during the ebb, as observed over similar large bedforms by Ernstsens et al. (2006).

The results from Experiment 5 show that changing morphology influences the FSZ. Changes of the FSZ observed during the flood are difficult to interpret due to the small size of the FSZ, which provided only a small amount of profiles to characterize the FSZ. During the ebb, the observed variations of the FSZ length are clearly related to changes in morphology. The normalized length of the FSZ varies by 1 to 2% for bedforms 1 and 3. For bedform 2 on the other hand, it varies by up to 10%, with minimal and maximal values of 5.2 and 6.1. More importantly, the position of the separation point clearly changes with changing bathymetry (Figure 7). In particular, it appears that at the beginning of the ebb, the flow separation point is situated relatively down on the lee side due to the gentle slope of the bed towards the crest. At the end of the ebb, sediment movement created a steeper slope at the crest and consequently, the flow separates at the crest.

Considering all experiments, FSZ is present over slip face angles between  $12$  and  $23^\circ$  and no FSZ is observed for smaller angles.

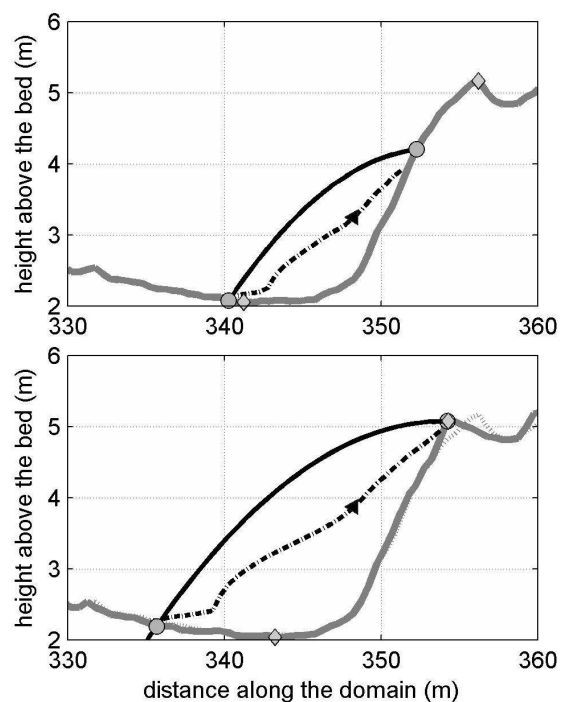


Figure 7. Detail of the FSZ over bedform 2 at the beginning (top) and at the end (bottom) of the ebb.

#### 4. DISCUSSION

The numerical experiments suggest that a permanent flow separation zone develops for lee side angles in excess of  $12^\circ$ . Although this value is smaller than those suggested by Kostaschuk and Villard (1996) and Best and Kostaschuk (2002) ( $19^\circ$  and  $>14^\circ$  respectively), it agrees well with the assumption of Paarlberg et al. (2009) that flow separation is permanent in time for a slope of  $10^\circ$  or more.

The experiments also show that variations of velocity and water level have no influence on the FSZ within the tested velocity range. This agrees with results from Paarlberg et al. (2007) who, based on results from a large dataset of previous lab experiments, did not find any relationship between length of FSZ and flow velocity or water depth. Importantly, our results suggest that tidal variations of water levels and velocities magnitude do not influence the FSZ.

The only variations of the FSZ are created by changes in the bed morphology, which is in line with the suggestion by Paarlberg et al. (2007) that the slope of the bed at the bedform crest is a critical parameter in determining the shape and length of the FSZ. The flow separation line was always well parameterized by a 3<sup>rd</sup> order polynomial, as proposed by Paarlberg et al. (2007); however, we found that the normalized length of the FSZ is on average between 5.5 and 6.2 which is much longer than the value of 5.2 that Paarlberg et al. (2007) calculated. The difference can be explained by the fact that the flume experiments all contained very few points in the FSZ which forced them to extrapolate velocity profiles, whereas we had on average 10 times more points available to precisely determine the length and shape of the FSZ. Furthermore, flume experimental settings usually use simple bedform shapes (typically a sinusoidal stoss side and a straight steep lee side) whereas we modeled large compound bedforms derived from field measurements.

#### 5. CONCLUSIONS

A non-hydrostatic numerical model was used to investigate the changes in the flow separation zone (FSZ) over natural compound bedforms in a

tidal environment. Several conclusions can be drawn from the model simulations:

- A permanent FSZ is observed on the steep lee sides of the bedforms during the ebb; whereas during the flood, no flow separation zone is generally observed except locally over the steepest part of the bed near the crest.
- Changes in velocity and water levels (steady or tidally-varying) do not affect the size of the FSZ.
- The size of the FSZ is influenced by changes in bed morphology during the tidal cycle, especially by the bed morphology around the crest.

#### 6. ACKNOWLEDGMENT

This study was funded through DFG-Research Center / Cluster of Excellence “The Ocean in the Earth System” and the Danish Council for Independent Research | Natural Sciences under the project “Process-based understanding and prediction of morphodynamics in a natural coastal system in response to climate change” (Steno Grant 10-081102).

#### 7. REFERENCES

- Best, J., 2005. The fluid dynamics of river dunes: A review and some future research directions. *Journal of Geophysical Research* 110 (F04S02): DOI 10.1029/2004JF000218.
- Best, J. & Kostaschuk, R., 2002. An experimental study of turbulent flow over a low-angle dune. *Journal of Geophysical Research* 107 (C9): DOI 10.1029/2000jc000294.
- Ernstsen, V., Noormets, R., Hebbeln, D., Bartholomä, A. & Flemming, B.W., 2006. Precision of high-resolution multibeam echo sounding coupled with high-accuracy positioning in a shallow water coastal environment. *Geo-Marine Letters* 26 (3): 141-149.
- Kostaschuk, R. & Villard, P., 1996. Flow and sediment transport over large subaqueous dunes: Fraser River, Canada. *Sedimentology* 43: 849-863.
- Lefebvre, A., Ernstsen, V.B. & Winter, C., 2011. Bedform characterization through 2D spectral analysis. *Journal of Coastal Research* SI64: 781-785.
- Lefebvre, A., Paarlberg, A.J. & Winter, C., 2012. A numerical investigation of flow separation over bedforms. Poster presented at the EGU General Assembly 2012, Vienna (Austria), 22-27 April 2012.

Lefebvre, A., Ernsten, V.B. & Winter, C., accepted. Estimation of roughness lengths and flow separation over compound bedforms in a natural tidal inlet. Continental Shelf Research.

McLean, S.R., Wolfe, S.R. & Nelson, J.M., 1999. Spatially averaged flow over a wavy boundary revisited. Journal of Geophysical Research 104 (C7): 15743-15753.

Paarlberg, A.J., Dohmen-Janssen, C.M., Hulscher, S.J.M.H. & Termes, P., 2007. A parameterization of flow separation over subaqueous dunes. Water

Resources Research 43: DOI 10.1029/2006WR005425.

Paarlberg, A.J., Dohmen-Janssen, C.M., Hulscher, S.J.M.H. and Termes, P., 2009. Modeling river dune evolution using a parameterization of flow separation. Journal of Geophysical Research 114 (F01014): DOI 10.1029/2007JF000910.

Vanoni, V.A. & Hwang, L., 1967. Relation Between Bed Forms and Friction in Streams. Journal of the Hydraulics Division: 121-144

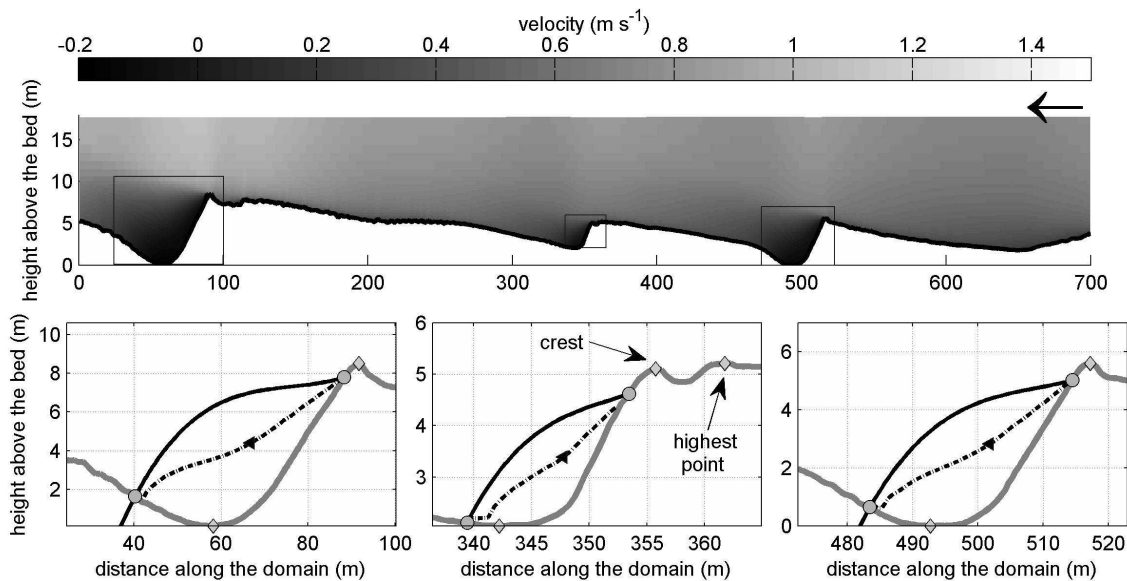


Figure 5. Velocities and FSZ over the 3 bedforms during maximum ebb velocity (see Figure 4 for details of the symbols). The arrow indicates the flow direction.

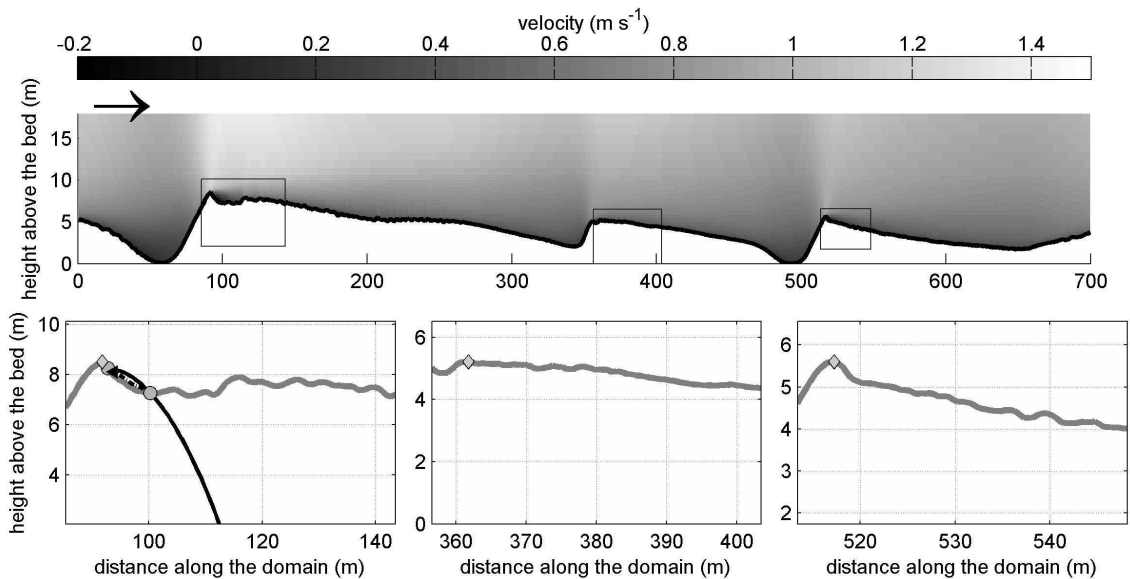


Figure 6. Velocities and FSZ over the 3 bedforms during maximum flood velocity (see Figure 4 for details of the symbols). The arrow indicates the flow direction.